

# Growth rate of the Rayleigh–Taylor instability in an ablatively accelerated inhomogeneous laser plasma

V. V. Bychkov, S. M. Gol'berg, and M. A. Liberman

*P. L. Kapitsa Institute of Physical Problems, Academy of Sciences of the USSR*

(Submitted 19 April 1991)

Zh. Eksp. Teor. Fiz. **100**, 1162–1185 (October 1991)

The growth of small instabilities during the ablative acceleration of planar foils by a laser light pulse is analyzed. It is shown that the question of the additional boundary conditions required for analytic solution of the problem in a model with a discontinuity front is related to the condition that the unperturbed flow be of an evolutionary nature. This question generally cannot be solved analytically. A scaling law is found and the corrections to the “classical” growth rate of the Rayleigh–Taylor instability for the finite density gradient, compressibility, convection, and the thermal conductivity of the plasma are calculated. Profiles of the hydrodynamic variables for a quasisteady unperturbed flow of the laser plasma found through a one-dimensional numerical simulation are used to derive a semiclassical solution of the spectral problem for the instability growth rates. The resulting solutions are compared with the solution of the spectral problem with the uniform-flow boundary conditions on both sides of the unstable region. They are also compared with the results of a two-dimensional numerical simulation. These comparisons show that the use of more-realistic boundary conditions leads to a higher instability growth rate. An intensification of the x-ray emission from the plasma corona or a decrease in the wavelength of the laser light causes significant improvements in the convective stabilization and in the stabilization due to the smoothing of the density profiles. A substantial decrease in the growth rates becomes possible for all instabilities.

## 1. INTRODUCTION

The Rayleigh–Taylor (RT) instability is one of the most important processes in the physics of high energy densities. In particular, in various schemes for achieving inertial fusion, the RT instability imposes a limit on the energy which can be introduced in order to initiate the reaction. Most schemes for laser fusion or beam fusion under consideration today involve some sort of extreme compression of shells with a large aspect ratio. If an extreme compression of this sort is to be possible, the target must retain a high degree of spherical symmetry throughout the compression process. Deviations from spherical symmetry in the course of the compression ultimately lead to a deviation from a spherical shape which is on the order of the instantaneous size of the target itself. The quantity  $\rho R$ , which increases as  $1/R^2$  in the case of spherically symmetric compression, stops increasing; i.e., the implosion comes to a halt. The degree of compression required under the assumption that the asymmetry grows at a constant rate can be achieved by using a target with a large initial radius, i.e., by substantially increasing the amount of energy which is delivered. Another consequence of the RT instability is mixing of the shell material and the fuel in the shell being compressed. Again, the result is to extinguish the reaction. This point is crucial from the standpoint of the amount of energy which can be introduced. While the irregularities in the irradiation are smoothed out to a large extent in the transverse direction by the electron thermal conductivity, the RT instability, being a hydrodynamic instability, is unavoidable during the compression of the plasma target and in this sense poses the greatest danger.

The classic RT instability arises at an interface between fluids at rest if a relatively heavy fluid (with a density  $\rho_h$ ) is being supported by a relatively light one (with a density  $\rho_l$ ).<sup>1,2</sup> In this case the growth rate of small perturbations with wave number  $k$  is  $\sigma = (Agk)^{1/2}$ , where

$$A = (\rho_h - \rho_l) / (\rho_h + \rho_l)$$

is the Atwood number, and  $g$  is the acceleration imparted to the heavy fluid. During the compression or acceleration of laser targets by a plasma, the gradients in the ablative pressure and the gradients in the density are in opposite directions near the ablation surface. In other words, the configuration is one in which the RT instability will occur. There is an important distinction, however, which arises because of the flow of mass and heat through the instability region and also because of the distributed smooth profiles of hydrodynamic properties. As recent experiments on laser ablative acceleration of plane foils have shown,<sup>3–7</sup> the growth rate of the most dangerous instability modes is smaller by a factor of about 2 or 3 than would be expected on the basis of the classical theory. In addition, at large values of  $k$ , i.e., in the short-wavelength region, the instability growth rates do not increase as they would be expected to do on the basis of the classical theory, but in fact vanish. Similar results emerge from two-dimensional numerical simulations of the growth of small perturbations which have been carried out<sup>8–12</sup> for both planar and spherical geometry. The growth rate of the RT modes found experimentally, like the results of the numerical simulation, agrees satisfactorily with the formula proposed by Takabe:<sup>13,14</sup>

$$\sigma = a(gk)^{1/2} - b(kv_a), \quad (1)$$

where  $v_a = \dot{m}_a / \rho_a$  is the velocity at which the plasma flows across the ablation front, and  $a$  and  $b$  are numerical coefficients. The results of 2D numerical simulations<sup>8,13</sup> show that the values of these coefficients are, quite accurately,  $a = 0.9$  and  $b = 3$ . The long-wavelength instabilities thus grow more slowly than the classical RT instabilities, and the modes which grow most rapidly correspond to the wave number

$$k_{\max} = \frac{a^2 g}{4b^2 v_a^2} = 0.02 \frac{g}{v_a^2}.$$

The corresponding growth rate is

$$\sigma_{\max} = \frac{a^2 g}{4b v_a} = 0,067 \frac{g}{v_a}.$$

Analytic and numerical models have been proposed in several places and have been used in efforts to explain the stabilization in the short-wavelength limit. These explanations have been based on the thermal conductivity and the flow of mass through the unstable region.<sup>15-24</sup> Although certain versions of the analytic work lead to a formula like (1) for the growth rate, the theory runs into a fundamental difficulty here, which we will discuss below.

In the present paper we are interested in the onset of the RT instability during the acceleration of planar targets by laser ablation. We derive analytic solutions for the spectrum of RT instabilities in the short-wavelength limit. We derive corrections for the compressibility, the thermal conductivity, and the convection. We discuss the hydrodynamic models which have been used in previous studies, the various formulations of the problems, and the choice of boundary conditions. We discuss the formulation of the eigenvalue problem, and we solve this problem. We derive the growth rates for the RT instability in the semiclassical approximation from the actual quasisteady profiles found for the various hydrodynamic properties through 1D numerical simulation of the problem of the ablative laser acceleration of an aluminum target.

Solving the eigenvalue spectral problem has several advantages over a 2D numerical simulation of the onset of an instability in a laser target,<sup>6,8</sup> in which case a Cauchy problem is examined for the growth of a given initial perturbation. The first advantage is that the spectral approach is not afflicted by an arbitrariness in the specification of the initial small perturbations. A second advantage is that the perturbation modes which grow most rapidly can easily be distinguished.

## 2. UNPERTURBED FLOW OF A LASER PLASMA

Let us examine the onset of instabilities during the laser acceleration of thin plane foils. The case of planar foils has the advantage over a spherical implosion of laser targets that both the theoretical and experimental studies on the processes accompanying the ablative acceleration of planar foils lead to a clearer understanding of the physical processes of most importance.<sup>25-28</sup> In the numerical calculations, realistic equations of state have been used. The heating of the target by x radiation, the radiation transport, etc., have been taken into account. We will make use of these calculations below in solving the overall spectral problem. To find the scaling and a simple analytic solution of the problem, it is sufficient to use a simpler model of hydrodynamic equations written in the c.m. coordinate system of the foil being accelerated. These equations are the continuity equation, the equation of motion, and the energy-transport equation:

$$\frac{\partial \rho}{\partial t} + \nabla(v\rho) = 0, \quad (2)$$

$$\rho \frac{\partial v}{\partial t} + \rho(\nabla v)v + \nabla P - \rho g_0 = 0, \quad (3)$$

$$\frac{\partial}{\partial t} \left[ \rho \left( \frac{1}{2} v^2 + \varepsilon \right) \right] + \nabla \left[ \rho v \left( \frac{1}{2} v^2 + W \right) - \kappa \nabla T \right] + I = \rho v g_0. \quad (4)$$

Here  $P$  is the plasma pressure;  $\kappa = \rho c_p \chi$  is the thermal conductivity;  $\varepsilon$ ,  $W$ , and  $c_p$  are the specific internal energy, the specific enthalpy, and the specific heat at constant pressure;  $I$  is the intensity of bulk sources of energy; and  $g_0$  is the acceleration of the center of mass of the foil.

After the laser pulse begins, a first shock wave propagates through the target. After this wave leaves the free rear surface of the target, the target particles begin a translational motion in the forward direction, parallel to the laser beam. A rarefaction wave propagates opposite the laser beam at the same time. After several reflections, a steady-state plasma flow is established.<sup>29-31</sup> In practice, a steady-state or self-similar plasma flow is established if the laser energy absorbed in the plasma becomes distributed over the plasma volume quickly in comparison with the hydrodynamic time

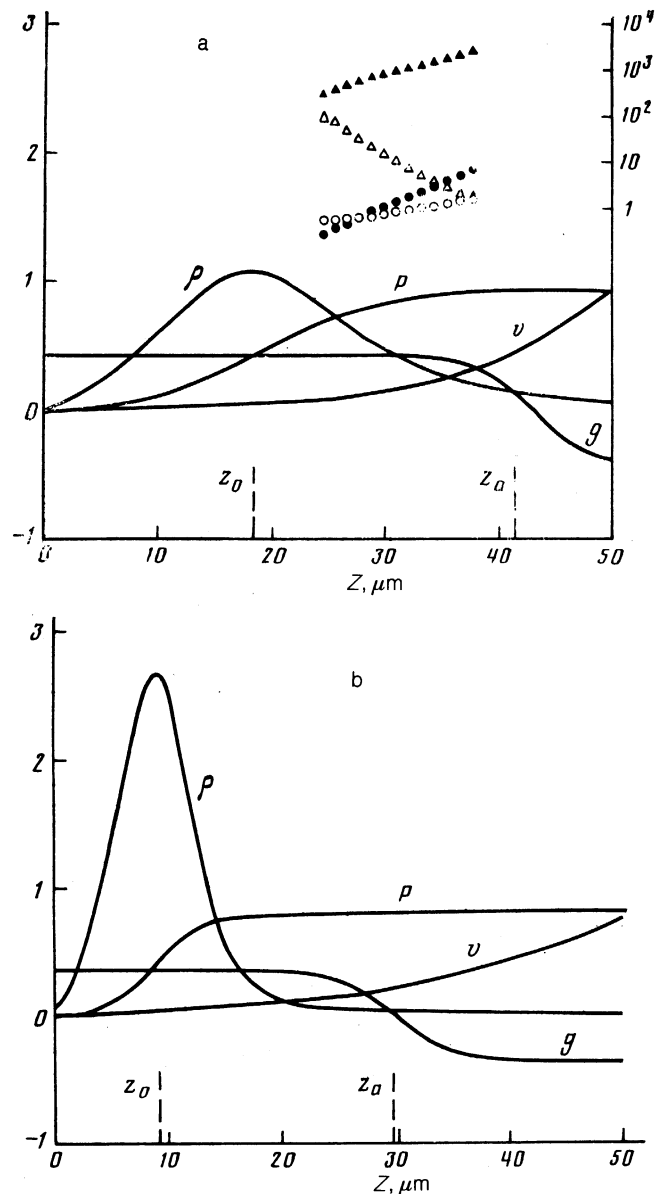


FIG. 1. Distributions of  $\rho$  ( $\text{g/cm}^3$ ),  $P$  (Mbar),  $v$  ( $10^6$  cm/s), and  $g$  ( $10^{15}$  cm/s<sup>2</sup>) in an ablatively accelerated plasma with  $I = 10^{13}$  W/cm<sup>2</sup>,  $\lambda = 1.06$   $\mu\text{m}$ ,  $d_0 = 10$   $\mu\text{m}$ , and  $\tau = 6$  ns. a: With allowance for x-ray emission from the plasma corona. ○—100 M<sup>2</sup>/Fr; ▲—100 M<sup>2</sup>/Fr; ●—Fr/Fr<sub>cr</sub>; Δ—Pe (the scale for these quantities is the logarithmic scale on the right). b: The x-ray emission from the plasma corona is suppressed.

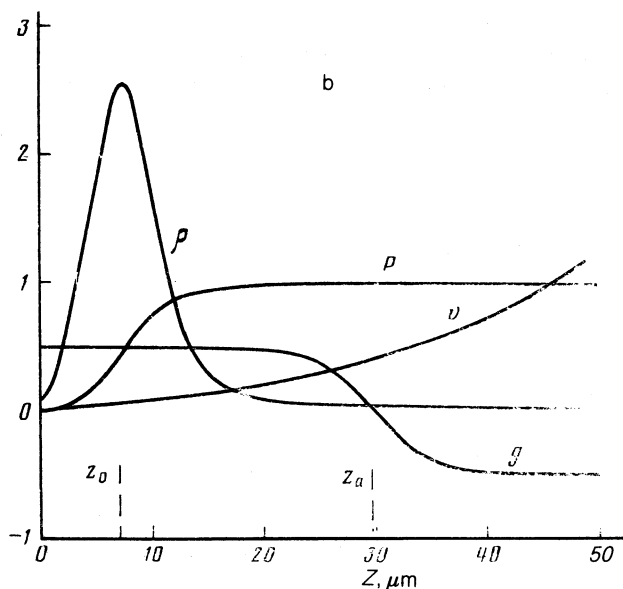
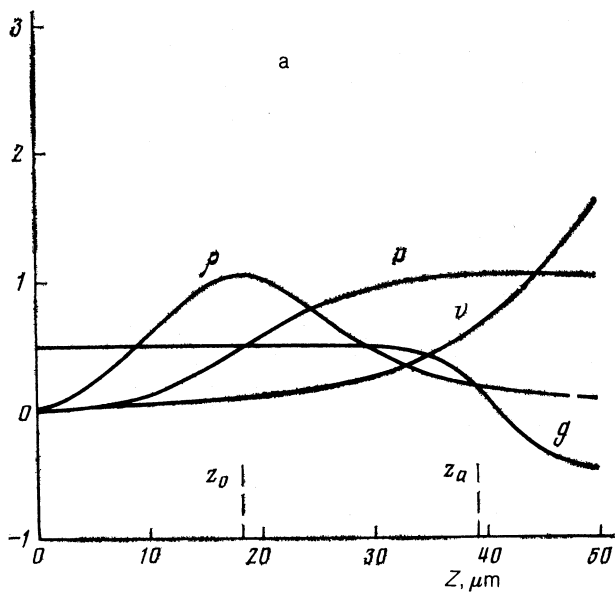


FIG. 2. Distributions of  $\rho$  ( $\text{g/cm}^3$ ),  $P$  (Mbar),  $v$  ( $10^6$  cm/s), and  $g$  ( $10^{15}$   $\text{cm/s}^2$ ) in an ablatively accelerated plasma with  $I = 10^{13}$   $\text{W/cm}^2$ ,  $\lambda = 0.26$   $\mu\text{m}$ ,  $d_0 = 10$   $\mu\text{m}$ , and  $\tau = 6$  ns. a—With x-ray emission from the plasma corona; b—this x-ray emission is suppressed.

scale of the flow. The time scale of the energy redistribution over the plasma volume is on the order of several times the time required for the rarefaction wave to propagate from the rear surface to the critical surface,  $\sim 2\text{--}3$  ns. A steady-state flow pattern like that in Figs. 1–3 then arises. We can distinguish three regions of this flow pattern: a plasma corona, which is expanding into the vacuum in the direction opposite the laser beam, from the critical surface where the density is  $\rho_c = \pi m_e m_i / Ze^2 \lambda_l^2$ , at which light with the wavelength  $\lambda_l$  is absorbed ( $e$  is the charge of an electron,  $m_e$  and  $m_i$  are the masses of an electron and an ion, and  $Z$  is the charge number of the plasma ion); the ablation zone, the region in which the heat absorbed in the corona is transferred by thermal conductivity to the denser layers of plasma; and the dense plasma which is actually being accelerated by the pressure of the ablation layer is the part of the target which has not evaporated.

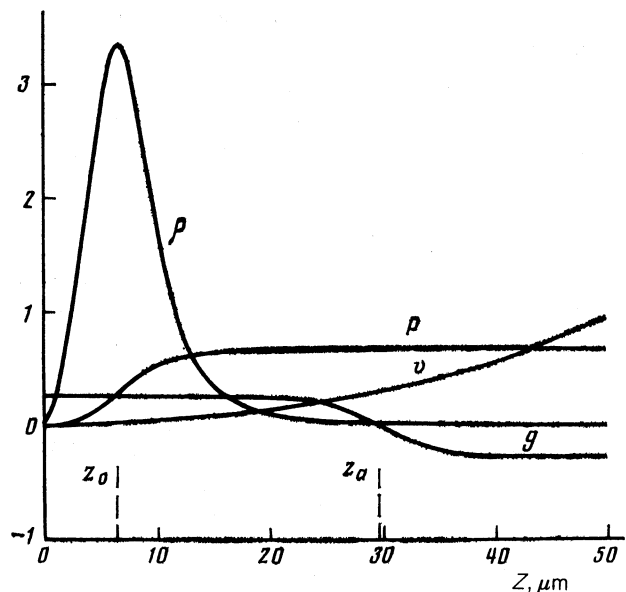


FIG. 3. Distributions of  $\rho$  ( $\text{g/cm}^3$ ),  $P$  (Mbar),  $v$  ( $10^6$  cm/s), and  $g$  ( $10^{15}$   $\text{cm/s}^2$ ) in an ablatively accelerated plasma with  $I = 5 \cdot 10^{12}$   $\text{W/cm}^2$ ,  $\lambda = 0.26$   $\mu\text{m}$ ,  $d_0 = 10$   $\mu\text{m}$ , and  $\tau = 6$  ns.

The acceleration of the center of mass of the plasma target can be estimated quite accurately in terms of the ablation pressure  $P_a$ :

$$g_0 = P_a / \rho_0 d_0 \quad (5)$$

( $d_0$  is the initial thickness of the target, and  $\rho_0$  is its initial density). The thickness of the ablation layer can be found from the value of the thermal diffusivity and the sound velocity  $c_{s0}$  at the critical surface:

$$d_a = \chi_c / c_{s0} \quad (6)$$

It follows from (6) that the thickness of the ablation layer is proportional to the wavelength of the laser light, and for typical experiments we would have  $d_a \approx 100$   $\mu\text{m} \gg d_0 \approx 10$   $\mu\text{m}$  for  $\lambda_l = 1.06$   $\mu\text{m}$  or  $d_a \approx d_0$  for  $\lambda_l = 0.26$   $\mu\text{m}$ . The nature of the unperturbed flow is determined by the values of two dimensionless parameters: the Péclet number  $Pe = vL / \chi$ , which characterizes the relative roles played by thermal conductivity and convection over a length scale  $\sim L$ , and the Froude number  $Fr = v^2 / gL$ , which characterizes the relative contribution of the inertial force and of convection.

The ablation zone, in which there is a steady-state heat transfer, gives way to the layer of accelerated plasma through a transition region, which is bounded on the left by the surface of maximum density (Fig. 1) and on the right by the surface at which the hydrodynamic acceleration

$$g = g_0 - \frac{\partial v}{\partial t} - v \frac{\partial v}{\partial z} \quad (7)$$

vanishes. The latter surface is naturally identified as the ablation front. In this transition region, the density decreases substantially ( $\rho_{\text{max}} / \rho_a > 10$ ), while the hydrodynamic acceleration remains essentially constant. This acceleration goes to zero rapidly at the ablation front. In a comparatively narrow transition region, with a width on the order of  $d_0$ , the condition for the onset of the RT instability,  $g \partial \rho / \partial z < 0$ , holds.

### 3. EIGENVALUE PROBLEM FOR THE HYDRODYNAMIC INSTABILITY OF A LASER PLASMA

To solve the problem of the growth of small perturbations, we linearize the initial system of hydrodynamic equations, writing all the hydrodynamic variables in the form

$$\varphi = \varphi_0 + \tilde{\varphi}, \quad (8)$$

where  $\varphi_0(z, t)$  is the exact solution for the unperturbed plasma flow. We write the small deviation  $\tilde{\varphi}$  in the following form for the case of planar geometry of the unperturbed flow:

$$\tilde{\varphi} = \tilde{\varphi}(z, t) \exp(ikx). \quad (9)$$

Knowing the solution of the eigenvalue problem, we can find the solution of the Cauchy problem for any initial perturbation, by writing this perturbation as a Fourier integral of the eigenfunctions of the spectral problem. The rise time of the instability is determined by the time evolution of the amplitude of the perturbation mode which is growing most rapidly.

Assuming that the perturbations are adiabatic, we write linearized equations for small perturbations:

$$\frac{\partial \tilde{\rho}}{\partial t} + \frac{\partial (v\tilde{\rho})}{\partial z} + \frac{\partial (\rho\tilde{v}_z)}{\partial z} + ik\rho\tilde{v}_x = 0, \quad (10)$$

$$\frac{\partial \tilde{v}_x}{\partial t} + v \frac{\partial \tilde{v}_x}{\partial z} = -ik \frac{\tilde{P}}{\rho}, \quad (11)$$

$$\frac{\partial \tilde{v}_z}{\partial t} + v \frac{\partial \tilde{v}_z}{\partial z} = -\frac{1}{\rho} \frac{\partial \tilde{P}}{\partial z} + \frac{\tilde{\rho}}{\rho} g - \tilde{v}_z \frac{\partial v}{\partial z}, \quad (12)$$

$$\frac{\partial \tilde{P}}{\partial t} + \gamma \tilde{P} \frac{\partial v}{\partial z} + v \frac{\partial \tilde{P}}{\partial z} + \tilde{v}_z \rho g + \gamma \tilde{P} \left( \frac{\partial \tilde{v}_z}{\partial z} + ik\tilde{v}_x \right) = 0. \quad (13)$$

Here  $\rho(z, t)$ ,  $v(z, t)$ ,  $g(z, t)$ , and  $P(z, t)$  are the profiles of the unperturbed flow, and the adiabatic index

$$\gamma = \left( \frac{\partial \ln P}{\partial \ln \rho} \right)_s$$

is determined for the unperturbed plasma from the actual equation of state. The derivation of Eqs. (10)–(13) did not require the assumption that the unperturbed flow is ideal in terms of its equation of state; nor were we obliged to assume that there was no dissipation, etc. The only assumptions were that the perturbations themselves are adiabatic and that there is a lower limit on the wavelength of the perturbations. It is easy to see that these limitations are not very important. For example, by requiring that the Peclet number for the perturbations be large, i.e.,

$$Pe(\lambda) = v\lambda/\chi \gg 1, \quad (14)$$

we find the limitation  $\lambda \gg l/M$ , on the perturbation wavelength, where  $l$  is the mean free path, and  $M$  the Mach number. For typical conditions we would have  $l = 10^{-3} \mu\text{m}$  and  $M = 10^{-1} - 10^{-2}$  and thus  $\lambda > 10^{-1} \mu\text{m}$ .

If the time scale for the variation of the properties of the unperturbed flow is  $\tau_{\text{un}}$ , we can use the semiclassical approximation for perturbations whose growth rate  $\sigma$  satisfies the inequality  $\sigma\tau_{\text{un}} \gg 1$ . We can introduce the concept of an "instantaneous growth rate" of the instability against the background of the given unperturbed plasma flow; here we would take  $\sigma$  to be the fastest of all the growth rates which characterize the various perturbation modes at the given instant.

The presence of modes which grow slowly in comparison with  $\exp(\sigma t)$  is unimportant, since these modes do not disrupt the symmetry of the unperturbed flow.

In the semiclassical approximation, the changes in the properties over the time  $t$  are given by the usual expression

$$\tilde{\varphi} = \tilde{\varphi}(z) \exp \left( \int_0^t \sigma(k, t') dt' \right). \quad (15)$$

The boundary conditions on Eqs. (10)–(13), in which the time derivatives are replaced by  $\sigma$  in the semiclassical approximation, follow from the requirement that the perturbations be regular. The choice of boundary conditions is determined by the particular formulation of the physical problem.

For laser acceleration of a thin foil in the steady state after the passage of the shock wave and the expansion wave, the rear surface of the target undergoes adiabatic expansion into vacuum in a gravitational field with an acceleration  $g_0$  (in the noninertial coordinate system of the center of mass of the plasma being accelerated). The conditions that the perturbations be regular at this surface then lead to the following asymptotic boundary conditions at the left-hand boundary as  $z \rightarrow 0$  (the asymptotic behavior of the properties of the unperturbed solution is

$$\rho \propto z^{1/(\gamma-1)}, \quad P \propto z^{1/(\gamma-1)+1}, \quad v = wz,$$

where  $w$  is a parameter of the profile:

$$\tilde{P} = h_p z^n, \quad \tilde{v}_x = h_x z^{n-1/(\gamma-1)}, \quad (16)$$

$$\tilde{v}_z = h_z z^{n-1/(\gamma-1)}, \quad \tilde{\rho} = h_r z^{n-1},$$

where

$$n = \frac{1}{2} \left( \frac{1}{\gamma-1} - \frac{\sigma}{w} \right) + \left[ \frac{1}{4} \left( \frac{1}{\gamma-1} - \frac{\sigma}{w} \right)^2 + \frac{1}{\gamma-1} \frac{\sigma}{w} + \frac{\gamma}{\gamma-1} \right]^{1/2}.$$

The coefficients  $h_z$ ,  $h_x$ , and  $h_r$  are expressed in terms of the coefficient  $h_p$ , which is arbitrary since the problem is linear, when  $\tilde{P}$ ,  $\tilde{v}_z$ ,  $\tilde{v}_x$ , and  $\tilde{\rho}$  from (16) are substituted into the linearized versions of Eqs. (10)–(13), with  $z \rightarrow 0$ .

On the right of the unstable region, in the ablation zone, the boundary conditions are the vanishing of the perturbations as  $z \rightarrow \infty$ , since we have  $kd_a \gg 1$ . This approach corresponds to imposing boundary conditions at  $z = z^*$  which satisfy the condition  $d_{\text{cr}} > z^* \gg d_a$ , where  $d_{\text{cr}}$  is the distance from the rear surface to the critical surface. In principle, the thickness  $d_a$  of the ablation zone can vary over a wide range, depending on the laser wavelength. Our calculations show, however, that the instability growth rate is essentially independent of the particular coordinate chosen as the right-hand boundary in the ablation zone.

The functions  $\rho(z, t)$ ,  $v(z, t)$ ,  $g(z, t)$ , and  $P(z, t)$ , which appear as coefficients in Eqs. (10)–(13), were found through numerical simulation of the 1D motion of an ablatively accelerated foil. The motion of the foil was simulated by means of the 1D Lagrangian hydrodynamic code "Impuls," which was described in Ref. 27. The calculation used the real equation of state.<sup>32</sup> The departure of the electron temperature from the ion temperature was taken into account. The

ionization kinetics was taken into account in the approximation of an average ion charge. The absorption of the laser light was calculated from the inverse bremsstrahlung mechanism. The electron thermal conductivity, which was limited with respect to the classical value in accordance with Ref. 33, and the x-ray emission, in the forward-backward approximation (25 energy groups), were incorporated in the energy transfer. The foil was partitioned into Lagrangian cells in such a way that there were at least 50 points in the ablation region in the quasisteady regime. This result was achieved by starting with a relatively fine mesh near the irradiated surface. The laser intensity reaches a steady-state value in 1 ns; the steady-state profiles are established in  $\sim 2$  ns.

Before we discuss the results of the solution of the spectral problem (10)–(13), we would like to examine some analytic approaches to the problem which make it possible to derive simple scaling relations and the behavior of the instability growth rate as a function of the parameters of the accelerated plasma and of the laser light. We recall that the “classical” expression for the growth rate of the instability of an interface between two incompressible fluids,  $\sigma = (Agk)^{1/2}$ , predicts an unbounded increase in the growth rate with increasing wave number  $k$ . In the problem under consideration here, however, the finite density gradient, the removal of mass from the instability region by convection, the thermal conductivity, and the compressibility lead to substantial—qualitative—changes in the instability growth rate.

#### 4. MODEL OF A UNIFORM FLOW WITH A DISCONTINUITY

In an effort to derive analytic solutions incorporating the convective flow of mass through the instability region, several studies<sup>15–21,23</sup> have used a model in which the unstable region in the ablation zone is replaced by discontinuity surface separating two uniform plasma flows. Despite the apparent simplicity of this model, attempts to derive a dispersion relation in it have run into a well known difficulty, the problem of the additional boundary conditions at the discontinuity front. Since this problem is of fundamental importance, we will discuss it here.

We assume that the inequalities

$$kc_s^2/g \gg 1, \quad \sigma c_s^2/gv \gg 1 \quad (17)$$

hold on the two sides of the unstable region. We also assume that the thickness of this unstable region is small in comparison with the length scales of the unperturbed flow. We can then think of the overall flow pattern as consisting of a discontinuity surface separating two uniform plasma flows, at  $z < 0$  and  $z > 0$ .

This picture of the unperturbed flow is similar to a deflagration wave, i.e., a subsonic combustion wave. For short-wavelength laser light, the critical surface is much closer to the ablation front, and the entire region out to the critical surface can be incorporated in the concept of the front. The flow in this case is similar to a deflagration wave with a supersonic flow behind the front.

A necessary condition for the existence of an unperturbed steady-state flow with a discontinuity is that the discontinuity be evolutionary.<sup>34</sup> This condition means that the number of boundary conditions at the front must be one greater than the number of independent perturbation modes

which can be radiated in either direction from the front. For a deflagration wave to be evolutionary, there must be an additional boundary condition—beyond the basic conditions which follow from the conservation of mass, momentum, and energy fluxes. This additional relation is the given propagation velocity of the deflagration front. In hydrodynamics, the propagation velocity of a deflagration front is given as an “external” parameter determined by the chemical kinetics, the calorific value of the fuel, etc. It follows in no way from the hydrodynamic equations. We run into a corresponding problem when we treat the ablation front as a discontinuity surface.

Writing the perturbations of all the hydrodynamic variables in the form  $\tilde{\varphi}(z,t) \propto \exp(\sigma t + \mu z)$ , solving Eqs. (10)–(13), and using the inequalities (17), we find the characteristic equation

$$(\sigma + v_i \mu)^2 \left[ (1 - M_i^2) \frac{\mu^2}{k^2} - 1 \right] = 0, \quad (18)$$

where the value  $i = 1$  specifies variables in the incoming flow ( $z < 0$ ), and the value  $i = 2$  specifies in the outgoing flow ( $z > 0$ ).

Using the inequalities (17) and the condition that the modes decay with distance from the front, we find that in the case of a subsonic unperturbed flow in the incoming region ( $i = 1, z < 0, M_1 = v_1/c_{s1} \ll 1$ ) only an acoustic mode is possible:

$$\tilde{v}_{sz} = \tilde{v}_s \exp(kz), \quad \tilde{v}_{sx} = i\tilde{v}_{sz}, \quad (19)$$

$$\tilde{P}_s = -\rho_1 \left( \frac{\sigma}{k} + v_1 \right) \tilde{v}_{sz}, \quad \tilde{\rho}_s = \frac{\tilde{P}_s}{c_{s1}^2}.$$

In the outgoing flow, at  $z > 0$ , there are three solutions which are linearly independent. They are the acoustic mode

$$\tilde{v}_{az} = \tilde{v}_a \exp \left[ -\frac{kz}{(1 - M_2^2)^{1/2}} \right], \quad \tilde{v}_{ax} = -i(1 - M_2^2)^{1/2} \tilde{v}_{az}, \quad (20)$$

$$\tilde{P}_a = \rho_2 \left[ \frac{\sigma}{k} (1 - M_2^2)^{1/2} - v_2 \right] \tilde{v}_{az}, \quad \tilde{\rho}_a = \frac{\tilde{P}_a}{c_{s2}^2},$$

the entropic mode

$$\tilde{\rho}_e = \tilde{\rho}_e \exp \left( -\frac{\sigma}{v_2} z \right), \quad \tilde{T}_e = -\frac{T_2}{\rho_2} \tilde{\rho}_e, \quad (21)$$

$$\tilde{v}_{ez} = \tilde{v}_{ex} = 0, \quad \tilde{P}_e = 0,$$

and the rotational (vorticity) mode

$$\tilde{v}_{vz} = \tilde{v}_v \exp \left( -\frac{\sigma}{v_2} z \right), \quad \tilde{v}_{vx} = -i \frac{\sigma}{v_2 k} \tilde{v}_{vz}, \quad (22)$$

$$\tilde{P}_v = 0, \quad \tilde{\rho}_v = 0.$$

The last two of these modes are carried along with the mass flow.

In the linear approximation, an arbitrarily small perturbation on both sides of the discontinuity is a linear combination of the modes (19)–(22) existing to the left and right of the discontinuity front. In this case the dispersion relation should be found from the boundary conditions on the matching of the corresponding solutions for the perturbations at the discontinuity surface at  $z = 0$ . These boundary conditions are the perturbations of the conservation equations for the mass, momentum, and energy fluxes, in which the perturbation of the coordinate of the discontinuity front,

$z = z_0(x, t)$ , should also be taken into account:

$$\Delta(\rho\tilde{v}_z + v\tilde{\rho} - \rho\sigma\xi) = 0, \quad (23)$$

$$\Delta(\tilde{P} + \tilde{\rho}v^2 + 2\rho v\tilde{v}_z + \rho g\xi) = 0, \quad (24)$$

$$\rho v\Delta(\tilde{v}_x + ikv\xi) = 0, \quad (25)$$

$$\Delta[\rho v^2\sigma\xi + \frac{1}{2}(v\tilde{P} + P\tilde{v}_z) + \frac{1}{2}v^3\tilde{\rho} + \frac{1}{2}\rho v^2\tilde{v}_z] = 0. \quad (26)$$

Here  $\Delta[\varphi] = \varphi_1 - \varphi_2$  is the jump in the corresponding property at the discontinuity surface, and  $\xi(x, t)$  is the perturbation of the position of the discontinuity front. For the perturbations we thus have<sup>15</sup>

$$\varphi(z, x, t) = \varphi_0 + \tilde{\varphi}(z, x, t) - \xi(x, t)\delta(z)\Delta\varphi. \quad (27)$$

We see that Eqs. (23)–(26) do not solve the problem. For the five perturbation amplitudes  $v_s, v_a, v_v, \rho_e$ , and  $\xi$  we have only four equations. This situation is a direct result of the evolutionary nature of the original unperturbed flow, which requires an additional boundary condition—in addition to the basic conditions which follow from the conservation laws.

In the problem of the stability of an interface between two fluids at rest, with different densities, this difficulty does not arise. For example, if for simplicity we adopt the incompressibility condition ( $M \ll 1, \sigma/c_s k \ll 1$ ) then we find the following results from Eqs. 23–26 with  $v_1 = v_2 = 0$ :

$$\Delta(\rho_0\tilde{v}_z - \rho_0\sigma\xi) = 0, \quad (28)$$

$$\Delta(\tilde{P} + \rho_0 g\xi) = 0, \quad (29)$$

$$\Delta\tilde{v}_z = 0. \quad (30)$$

Although the number of boundary conditions has been lowered by one in the case  $v = 0$  [see Eq. (25)], in a fluid at rest we also lose the two modes in (21) and (22), which are carried along with the mass flow. Using (19) and (20), we can then immediately find a dispersion relation for the classical RT instability from Eqs. (28)–(30):

$$\sigma^2 = gk \frac{\rho_1 - \rho_2}{\rho_1 + \rho_2}. \quad (31)$$

Formally, a dispersion relation could be found in the case  $v \neq 0$  if we had some relation among the perturbation amplitudes to supplement Eqs. (23)–(26). Possible versions of this additional relation were discussed in Refs. 15–23, but this additional relation is “external” with respect to the model discussed in the hydrodynamic approach, as we have already mentioned. The choice of this relation is “a matter of taste.” At the same time, this model of uniform flows as  $z \rightarrow \pm \infty$  makes it possible to find an “exact” dispersion relation by a numerical simulation in which the discontinuity is replaced by a transition region with a known structure. The condition that the unperturbed flow be evolutionary is a necessary condition for the existence of a steady-state structure of the discontinuity front.<sup>34</sup> At a formal level, specifying the structure of the discontinuity is equivalent to imposing an additional boundary condition.

The case of a supersonic flow out of the discontinuity surface at  $z > 0$  was also studied in Ref. 19. The condition that a deflagration wave of this sort be evolutionary would require two additional boundary conditions.<sup>34</sup> Correspondingly, to close the equations for the amplitudes and to derive a dispersion relation, we would require two relations in addi-

tion to (23)–(26), since in this case we have an additional acoustic mode at  $z > 0$ .

## 5. GROWTH RATES OF THE RT INSTABILITY FOR NONUNIFORM DISTRIBUTIONS OF THE ACCELERATION AND THE DENSITY

We consider an ideal plasma at rest, with nonuniform distributions of the density, the pressure, and the acceleration along the  $z$  axis.

Adopting perturbations in the form

$$\tilde{\varphi} = \tilde{\varphi}(z) \exp(\sigma t + ikx), \quad (32)$$

with  $v = 0$ , we can reduce Eqs. (10)–(13) to a single equation for  $\tilde{v}_z$ :

$$\frac{d}{dz} \left[ \frac{\rho\sigma^2\gamma P}{\rho\sigma^2 + k^2\gamma P} \frac{d}{dz} \tilde{v}_z \right] - \left[ \rho\sigma^2 + g \frac{d\rho}{dz} - \frac{\rho^2 g^2 k^2}{\rho\sigma^2 + k^2\gamma P} - \frac{d}{dz} \left( \frac{\rho^2 g\sigma^2}{\rho\sigma^2 + k^2\gamma P} \right) \right] \tilde{v}_z = 0. \quad (33)$$

The boundary conditions follow from the continuity of the velocity and pressure perturbations in the fluid particles. In particular, we have  $\tilde{v}_z = 0$  at rigid boundaries or in the limit  $z \rightarrow \pm \infty$  if there are no boundaries.

Since the pressure perturbation in Lagrangian coordinates is

$$\tilde{P}_{\text{Lagr.}} \propto \rho \left( -\frac{d}{dz} \tilde{v}_z + \frac{gk^2}{\sigma^2} \tilde{v}_z \right) \propto \gamma P \nabla \tilde{v}, \quad (34)$$

it is easy to see that if there is a free surface “below,” at which the density vanishes and the relation  $gd\rho/dz < 0$  holds, then Eq. (33) with  $g = \text{const}$  has a solution corresponding to a “global” mode of the RT instability:  $\tilde{v}_z \propto \exp(kz)$ . This solution satisfies Eq. (33) with  $\nabla \cdot \tilde{v} = 0$  regardless of the density profile  $\rho(z)$  (Refs. 35 and 36). The global mode of the RT instability has the highest growth rate,  $\sigma^2 = gk$ .

To study the behavior of the growth rate as a function of the density profile, we consider the limit of an incompressible fluid. Equation (33) becomes

$$\frac{d^2}{dz^2} \tilde{v}_z - \alpha(z) \frac{d}{dz} \tilde{v}_z - k^2 \left( 1 - \frac{g\alpha(z)}{\sigma^2} \right) \tilde{v}_z = 0, \quad (35)$$

where  $\alpha(z) = -d(\ln(\rho))/dz$  is the steepness of the density profile.

Equation (35) can be solved easily when a layer of fluid with an exponentially decreasing density  $\rho \propto \exp(-\alpha z)$  in a uniform gravitational field  $g = \text{const} > 0$  is bounded by walls at  $z = 0$  and  $L$ :

$$\tilde{v}_z \propto \exp\left(\frac{\alpha}{2} z\right) \sin\left(n \frac{\pi}{L} z\right). \quad (36)$$

Here  $n$  is the index of the wave eigenfunction. The dispersion relation corresponding to the solution (36) is

$$\sigma_n^2(k) = \frac{g\alpha}{1 + \alpha^2/4k^2 + n^2\pi^2/k^2L^2}. \quad (37)$$

Approximating the arbitrary distribution of the density by a finite number of layers with an exponential density distribution  $\rho_i \propto \exp(-\alpha_i z)$  in each layer  $i$ , we can show that in the short-wavelength limit

$$kL_i \gg 1, \quad k/\alpha_i \gg 1 \quad (38)$$

the instability growth rate has the asymptotic form (36), (37), where  $\alpha = \max_i(\alpha_i)$  and  $L$  are respectively the steepness and thickness of the layer of maximum steepness. The eigenfunction is localized in the layer of maximum steepness in this case and falls off exponentially outside this layer, in accordance with

$$\exp\left[-\left(\frac{\alpha-\alpha_i}{\alpha}\right)^{1/2} kz\right]. \quad (39)$$

For any finite wave number  $k$  we find the following estimate. If the function

$$f_\alpha(k) = \frac{g\alpha}{1+\alpha^2/4k^2}$$

for layer  $j$  takes on a value which is the highest value in terms of  $\alpha$ , then one can show that the following inequality holds for the growth rate of the RT instability for the given  $k$ :

$$\frac{g\alpha_j}{1+\alpha_j^2/4k^2+\pi^2/k^2L_j^2} < \sigma^2 < \frac{g\alpha_j}{1+\alpha_j^2/4k^2}. \quad (40)$$

For an arbitrary discontinuous density profile with a steepness  $\alpha < \alpha_{\max}$ , the growth rate of the RT instability is then limited by the inequality

$$\sigma^2 < \frac{g\alpha_{\max}}{1+\alpha_{\max}^2/4k^2} \quad \text{for } k > \frac{1}{2}\alpha_{\max},$$

$$\sigma^2 < gk \quad \text{for } k < \frac{1}{2}\alpha_{\max}, \quad (41)$$

where  $gk$  is the envelope of the single-parameter family of functions  $f_\alpha(k)$ .

We can estimate the effect of nonuniformity of the acceleration  $g(z)$  similarly. In the approximation of an incompressible fluid with a continuous density profile  $\rho(z)$  and a nonuniform acceleration  $g(z)$ , the instability modes with the maximum growth rate are localized in a layer  $L^*$ , in which we have  $g(z)\alpha(z) \approx \max(g\alpha)$ . In the limit of large wave numbers the growth rate is given by

$$\sigma^2 = \frac{\max(g\alpha)}{1+(\alpha^*/2k)^2+(\pi/kL^*)^2}, \quad (42)$$

where  $\alpha^* = -d(\ln(\rho))/dz$  in layer  $L^*$ .

## 6. CONVECTIVE STABILIZATION

The effect of the plasma flow velocity on the instability growth rate in the short-wavelength limit can be estimated by perturbation theory, as small corrections in terms of the Froude number  $Fr = v^2\alpha/g$ , which characterizes the role of convection in the plasma being accelerated.

We assume

$$Fr \ll \alpha^2/k^2 \ll 1, \quad (43)$$

i.e., that the velocity of the unperturbed flow is small in the unstable region.

We write Eqs. (10)–(13) for small perturbations in the approximation of an ideal incompressible fluid:

$$\left(\sigma + v \frac{d}{dz}\right) \bar{\rho} - \rho \alpha \tilde{v}_z + \bar{\rho} \frac{d}{dz} v = 0, \quad (44)$$

$$\left(\sigma + v \frac{d}{dz}\right) \frac{d}{dz} \tilde{v}_z = -k^2 \frac{\bar{P}}{\rho}, \quad (45)$$

$$\left(\sigma + v \frac{d}{dz}\right) \tilde{v}_z = -\frac{1}{\rho} \frac{d}{dz} \bar{P} + \frac{\bar{\rho}}{\rho} g - \tilde{v}_z \frac{d}{dz} v, \quad (46)$$

$$ik\tilde{v}_x + \frac{d}{dz} \tilde{v}_z = 0. \quad (47)$$

For a fluid at rest ( $Fr = 0$ ), Eqs. (44)–(47) reduce to Eq. (35) which we write in the form

$$\hat{R}\tilde{v}_z + S_0\rho\tilde{v}_z = 0, \quad (48)$$

where

$$\hat{R} = \frac{1}{k^2} \frac{d}{dz} \left( \rho \frac{d}{dz} \right) - \rho$$

is a self-adjoint differential operator with the eigenvalues  $S_{0n} = g\alpha/\sigma_n^2$  [see (37)], as follows immediately from (35) for the eigenfunctions (36).

To within small terms in an expansion in powers of  $(Fr)^{1/2}$ , we find the following equation from Eqs. (44)–(47):

$$\hat{R}\tilde{v}_z + S_0\rho\tilde{v}_z - \rho\hat{W}\tilde{v}_z = 0. \quad (49)$$

The operator

$$\hat{W} = \frac{2v}{\sigma} \frac{d}{dz} + \frac{1}{\sigma} \left( 2 \frac{dv}{dz} + v\alpha \right) \quad (50)$$

is a small correction to the unperturbed operator  $\hat{R}$  in terms of  $(Fr)^{1/2}$  with  $\sigma \sim (g\alpha)^{1/2}$ , and the boundary conditions are expressed as an exponential decay outside the interval  $(0, L)$ .

We accordingly seek the eigenvalues and eigenfunctions of the operator (49) in the form

$$S_n = S_{0n} + S_{1n} + S_{2n} + \dots, \quad (51)$$

$$\tilde{v}_z^{(n)} = \sum_m c_m^{(n)} \tilde{v}_{zm}, \quad (52)$$

where the eigenfunctions  $\tilde{v}_{zm}$  are solutions of Eq. (48) for the eigenvalues

$$S_{0m} = 1 + m^2 \frac{\pi^2}{k^2 L^2} + \frac{\alpha^2}{4k^2}$$

and  $c_m^{(n)} = c_{m0}^{(n)} + c_{m1}^{(n)} + \dots$ . Using the standard technique of perturbation theory,<sup>38</sup> we find the following result for the first-order correction to the lowest eigenvalue,  $S_{01}$ , which corresponds to the maximum growth rate in the case  $n = 1$ :

$$S_{11} = (\rho\hat{W})_{11}, \quad (53)$$

where

$$(\rho\hat{W})_{m1} = \left( \int_0^L \tilde{v}_{zm} \rho \hat{W} \tilde{v}_{z1} dz \right) \left( \int_0^L \rho \tilde{v}_{zm}^2 dz \right)^{-1/2} \left( \int_0^L \rho \tilde{v}_{z1}^2 dz \right)^{-1/2}. \quad (54)$$

Correspondingly, for the second-order corrections we find

$$S_{21} = - \sum_{n=2} \frac{(\rho\hat{W})_{1n} (\rho\hat{W})_{n1}}{S_{0n} - S_{01}}. \quad (55)$$

To estimate the corrections to the instability growth rate, we set  $v = \text{const}$  and evaluate the integrals in (53) and (55). As a result we find

$$S_{11} = 2v\alpha/\sigma = 2(Fr)^{1/2}, \quad (56)$$

$$S_{21} = \frac{v^2 k^2}{\sigma^2} \frac{1}{\pi^2} \sum_{n=1} \frac{256n^2}{(4n^2-1)^3} = \frac{9,8}{\pi^2} \frac{k^2}{\alpha^2} Fr. \quad (57)$$

The instability growth rate can thus be written in the following form, to within terms of second order in perturbation theory:<sup>1)</sup>

$$\sigma^2 = \frac{g\alpha}{1 + \alpha^2/4k^2 + \pi^2/k^2L^2} \left[ 1 - 2(\text{Fr})^{1/2} - \frac{k^2}{\alpha^2} \text{Fr} \right]. \quad (58)$$

Expression (58) obviously does not give us a complete solution of the spectral problem—the behavior of the instability growth rate for all wavelengths—but it does give a fairly accurate description of the behavior of the growth rate near the maximum at small values of Fr. The maximum growth rate is

$$\sigma_{\max}^2 = g\alpha \left\{ 1 - (\text{Fr})^{1/2} \left[ 2 + \left( 1 + 4 \frac{\pi^2}{\alpha^2 L^2} \right)^{1/2} \right] \right\}. \quad (58a)$$

From (37) and (58) we find that the instability growth rate does not exceed  $(g\alpha)^{1/2}$ . Consequently, approximating of the growth rate by (1) may be valid if the growth rate reaches its maximum value at

$$k_{\max} = \frac{a^2 g}{4b^2 v^2} = \alpha \frac{a^2}{4b^2} \frac{1}{\text{Fr}} \ll \frac{\alpha}{2}.$$

Correspondingly, with  $b = 3$ , this means

$$\text{Fr} > \text{Fr}_{\text{cr}} \approx 0,06. \quad (59)$$

Expressions (58) and (58a) are a good approximation for  $\text{Fr} < \text{Fr}_{\text{cr}}$ , while (58) is a good approximation for  $\text{Fr} > \text{Fr}_{\text{cr}}$  (Fig. 4).

To estimate Fr, we can assume, in order of magnitude,

$$g \approx \frac{P_a}{\rho_0 d_0}, \quad \alpha \approx \frac{2}{d_0}, \quad v \approx \frac{\rho_c}{\rho_0} v_c,$$

where  $v_c$  is the plasma velocity at the critical surface. We then find the Froude number to be

$$\text{Fr} \approx \rho_c / 2\rho_0. \quad (60)$$

In particular, from (60) we find  $\text{Fr} \approx 0,02$  for a target accel-

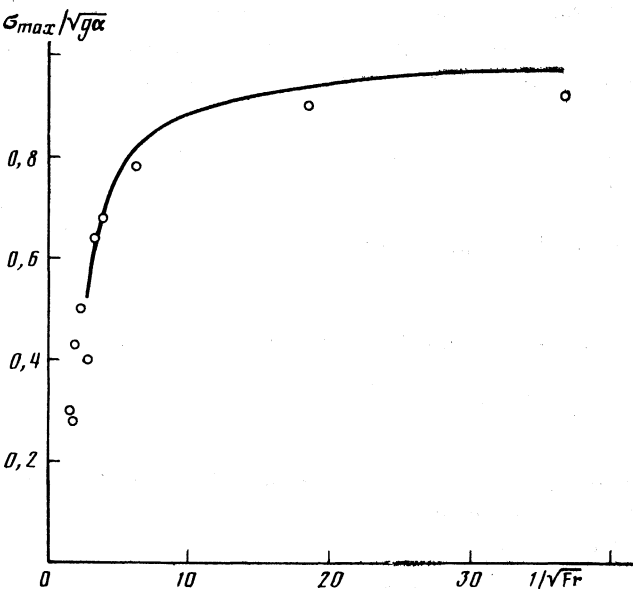


FIG. 4. Maximum instability growth rate as a function of  $1/(\text{Fr})^{1/2}$ . [ $\text{Fr} = \text{Fr}(\alpha_{\max})$ ].

erated ablatively by light with  $\lambda_l = 1.06 \mu\text{m}$  from a Nd laser. This result agrees satisfactorily with the results of numerical calculations.

We thus see that irradiation by higher harmonics of the laser light reduces the growth rate of the RT instabilities in the accelerated plasma by convection to a greater extent.

Typical values of  $\text{Fr}/\text{Fr}_{\text{cr}}$  in the instability localization region  $(z_0, z_a)$ , found from the results of 1D numerical simulation of the ablative acceleration of Al targets under various conditions, are shown in Fig. 1a.

Figure 4 shows values of the maximum instability growth rates, normalized to  $(g\alpha)^{1/2}$ , for various values of the characteristic number Fr. These results were calculated for the interval  $(z_0, z_a)$  from the solution of the complete spectral problem for various regimes of the unperturbed flow of an ablatively accelerated plasma. We see from Fig. 4 that the behavior of  $\sigma_{\max}/(g\alpha)^{1/2}$  as a function of Fr agrees well with the asymptotic expression (58a) up to values  $\text{Fr} > \text{Fr}_{\text{cr}} \approx 0,06$ , and it agrees well with the asymptotic behavior for Takabe's approximate expression (1):  $\sigma_{\max}/(g\alpha)^{1/2} \propto 1/(\text{Fr})^{1/2}$  at large values of the Froude number.

## 7. EFFECT OF COMPRESSIBILITY AND THERMAL CONDUCTIVITY ON THE INSTABILITY GROWTH RATE

The role played by the plasma compressibility is characterized by two parameters:<sup>18</sup> the Mach number  $M = v/c_s$  (the sound velocity is  $c_s^2 = \gamma P/\rho$ ), which characterizes the compressibility of the plasma flow carrying particles out of the instability region, and the "acoustic" Froude number in the unstable region,  $\text{Fr}_s = c_s^2 \alpha/g = \text{Fr}/M^2$ , which determines the actual effect of the compressibility on the growth rate of the RT instability with respect to the growth rate in a fluid at rest. Figure 1a shows typical values of  $M^2$  and  $\text{Fr}_s$  found by numerical simulation in the region  $(z_0, z_a)$ .

Introducing the parameter  $\delta = \sigma/c_s^2 k^2$ , which vanishes in the short-wavelength limit, we can rewrite Eq. (33) for small perturbations in a fluid at rest as follows:

$$\frac{1}{k^2} \frac{d}{dz} \left( \frac{\rho}{1+\delta} \frac{d}{dz} \tilde{v}_z \right) - \rho \left[ 1 - \frac{g\alpha}{\sigma^2} - \frac{1}{1+\delta} \frac{g^2}{c_s^2 \sigma^2} - \frac{1}{\rho} \frac{d}{dz} \left( \frac{\rho}{1+\delta} \frac{g}{c_s^2 k^2} \right) \right] \tilde{v}_z = 0. \quad (61)$$

In the short-wavelength limit,  $\alpha/k \ll 1$ , Eq. (61) becomes

$$\frac{1}{k^2} \frac{d}{dz} \left( \rho \frac{d}{dz} \tilde{v}_z \right) - \rho \left[ 1 - \frac{g\alpha}{\sigma^2} \left( 1 + \frac{1}{\text{Fr}_s} \right) \right] \tilde{v}_z = 0. \quad (62)$$

The solution of the spectral problem in the short-wavelength limit is

$$\sigma^2 = \frac{g\alpha}{1 + \alpha^2/4k^2 + \pi^2/k^2L^2} \left( 1 + \frac{1}{\text{Fr}_s} \right). \quad (63)$$

In other words, the corrections to the growth rate for the compressibility are determined by the quantity  $(1/\text{Fr}_s)$ , which is generally not small.

The corrections for the compressibility of the unperturbed flow are small, proportional to  $M^2$ . For acoustic perturbation modes in the approximation of a discontinuity and a uniform flow, for example, the spatial distribution (19) is

replaced by  $\exp(\pm kz/(1-M^2)^{1/2})$ . The corresponding corrections for the compressibility in expression (58) can be estimated to be

$$\sigma^2 = g\alpha \left[ 1 + \frac{1}{Fr_s} - 2 \left( \frac{Fr}{1+1/Fr_s} \right)^{1/2} - \frac{k^2}{\alpha^2} \frac{Fr}{(1+1/Fr_s)(1-M^2)} \right]. \quad (64)$$

As we have already mentioned, the corrections to the growth rate for the finite thermal conductivity can be important only in the short-wavelength limit. To estimate the effect of finite thermal conductivity in comparison with that of convection, we consider the equations for the perturbations in the approximation of an incompressible plasma at rest under the condition

$$\frac{\chi k^2}{(g\alpha)^{1/2}} \ll \frac{\alpha^2}{k^2} \ll 1. \quad (65)$$

From the linearized versions of the heat-conduction equation, the continuity equation, and the equation of motion, in which we retain terms up to first order in the small parameter (65), we find

$$\frac{1}{k^2} \frac{d}{dz} \left( \rho \frac{d}{dz} \tilde{v}_z \right) - \rho \left[ 1 - \frac{g\alpha}{\sigma^2} \left( 1 - \frac{\chi k^2}{\sigma} \right) \right] \tilde{v}_z = 0. \quad (66)$$

Calculating the growth rate, we find, in the short-wavelength limit,

$$\sigma^2 = \frac{g\alpha}{1 + \alpha^2/4k^2 + \pi^2/k^2 L^2} \left[ 1 - \frac{\chi k^2}{(g\alpha)^{1/2}} \right]. \quad (67)$$

Comparing the correction for the thermal conductivity in (67) with the correction [in (58)] for convection, we easily see that the thermal conductivity is relatively unimportant under the condition  $Pe = \nu/\chi\alpha \gg 1$ . The typical values of the  $Pe$  number found from the numerical calculations (Fig. 1a) show that the thermal conductivity is generally inconsequential.

## 8. SOLUTION OF THE SPECTRAL PROBLEM

As we mentioned back in Sec. 4, it is essentially impossible to derive an analytic solution of the spectral problem for RT instabilities in the case with convective transport of particles, even in a very simple model with a discontinuity. On the other hand, the spectral problem (10)–(13) can be solved numerically as an eigenvalue problem. In the semiclassical approximation, the coefficients  $v(z,t)$ ,  $\rho(z,t)$ ,  $P(z,t)$ , and  $g(z,t)$  in Eqs. (10)–(13) are treated as steady-state profiles of the unperturbed flow found through a 1D numerical simulation of the original problem of the ablative acceleration of a foil by a laser light pulse. Quasisteady profiles are established after the passage of several shock waves and rarefaction waves following the beginning of the laser pulse. The typical  $v(z)$ ,  $\rho(z)$ ,  $P(z)$ , and  $g(z)$  profiles in Figs. 1–3 were found in numerical calculations at  $t = 6$  ns, at which point the plasma flow was essentially in a quasisteady state.

In the numerical solution, eigenvalues of the problem (10)–(13) for perturbations as in (32) were sought by a "shooting" method. For a given approximation  $\sigma^{(k)}$ , the system of differential equations was solved by the Adams method, and then a new value  $\sigma^{(k+1)}$  was found by New-

ton's method:

$$\sigma^{(k+1)} = \sigma^{(k)} - F(\sigma^{(k)}) (dF/d\sigma)^{-1}.$$

The value of  $dF/d\sigma$  was found numerically. Here  $F(\sigma) = 0$  is the boundary condition at the right-hand boundary, at  $z = z^*$ :

$$F(\sigma) = \left\{ i\tilde{v}_z + \frac{k\bar{P}}{\sigma\rho} - \frac{\sigma}{vk} \tilde{v}_z + \left[ \frac{e_s}{(1-M^2)^{1/2}} \left( \frac{\sigma}{vk} + \frac{vk}{\sigma} \right) - 2 \right] Y \right\} \Big|_{z=z^*} = 0, \quad (68)$$

where

$$Y = \frac{c_s^2}{h_y(1-d_h c_s^2)} (\bar{\rho} - d_h \bar{P}), \quad d_h = \frac{\sigma}{vg} \left( \frac{v^2 k^2}{\sigma^2} - 1 \right),$$

$$h_y = \rho v \left[ \frac{\sigma}{vk} - \frac{e_s}{(1-M^2)^{1/2}} \right],$$

$$e_s = \left[ 1 + \frac{\sigma^2}{c_s^2 k^2} + \frac{1}{1-M^2} \left( M \frac{\sigma}{c_s k} + \frac{g}{c_s^2 k} \right)^2 \right]^{1/2} + \frac{1}{(1-M^2)^{1/2}} \left( M \frac{\sigma}{c_s k} + \frac{g}{c_s^2 k} \right).$$

The iterative process was terminated when the following condition was satisfied:

$$(\sigma^{(k+1)} - \sigma^{(k)})/\sigma^{(k)} < 0.005.$$

A check was then made to see whether the inequality

$$F(1.01\sigma^{(k+1)}) \cdot F(0.99\sigma^{(k+1)}) < 0$$

was satisfied.

In the solution of Eqs. (10)–(13), the integration away from the singular point  $z = 0$  was performed in accordance with the asymptotic behavior (16). The value of  $z_{\min}$  from which the system of differential equations was actually solved was chosen in the interval  $(0.02-0.05)z_0$ , where the coordinate  $z_0$  corresponds to the density maximum. The calculations showed that the value found for  $\sigma$  is essentially independent of the value of  $z_{\min}$  over the specified interval.

Figure 5 shows the perturbation growth rate,  $\sigma = \sigma(k)$ , found through the solution of the spectral eigenvalue problem (10)–(13) with boundary conditions (16) and (68), for the unperturbed flow of ablatively accelerated plasma corresponding to Figs. 1a and 2a.

We see from Fig. 5 that as we go to progressively shorter laser wavelengths the instability mode which grows most rapidly shifts in the long-wavelength direction in the  $\sigma(k)$  dispersion relation. Specifically, we find  $\lambda_{\max} \approx 25 \mu\text{m}$  at  $\lambda_l = 0.26 \mu\text{m}$  and  $\lambda_{\max} \approx 16 \mu\text{m}$  at  $\lambda_l = 1.06 \mu\text{m}$ . The instability growth rate at  $\lambda = \lambda_{\max}$  is 30–40% lower when the target is irradiated with the fourth harmonic of the laser than when it is irradiated with the first harmonic, under otherwise equal conditions. A substantially greater decrease in the instability growth rate as we switch to shorter laser wavelengths occurs in the short-wavelength part of  $\sigma(k)$ .

The x radiation from the plasma corona heats the dense layers of the plasma of the accelerated part of the target to a greater or lesser extent, depending on the intensity of this radiation. A relatively high intensity of the x radiation and a correspondingly pronounced heating of the dense plasma lead to the density profiles with a gentler slope, while they

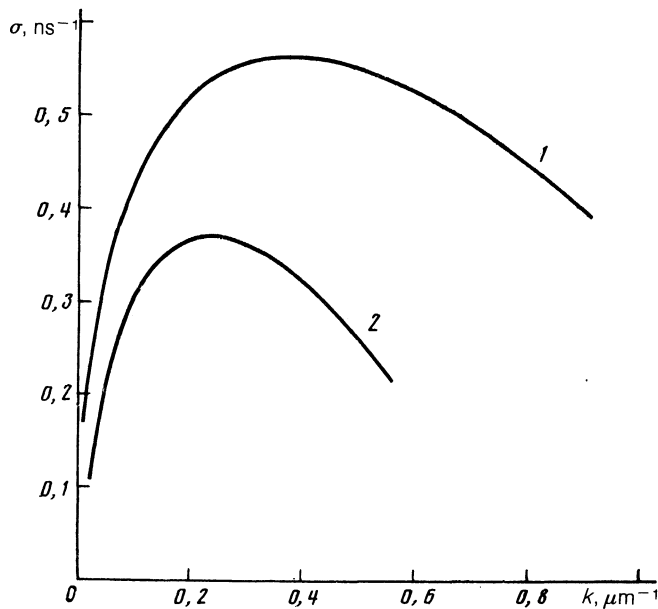


FIG. 5. Instability spectra for the ablative acceleration of an Al target for unperturbed flows corresponding to the profiles in Figs. 1a (curve 1) and 2a (curve 2).

increase the convection of particles out of the instability region ( $z_0, z_a$ ) (compare Figs. 1a, b, and 2a, b). By preparing a target with multilayer coatings of materials with different values of  $Z$ , and by varying the intensity of the x-ray emission from the plasma corona, one can thus alter the dynamics and growth rate of the instabilities in the course of the ablative acceleration of targets.

Figures 6 and 7 show the perturbation growth rate,  $\sigma = \sigma(k)$ , found through a solution of the spectral problem (10)–(13) for unperturbed flows under the conditions corresponding to Figs. 1a, b, and 2a, b, respectively. In the numerical simulation of the ablatively accelerated foil in ver-

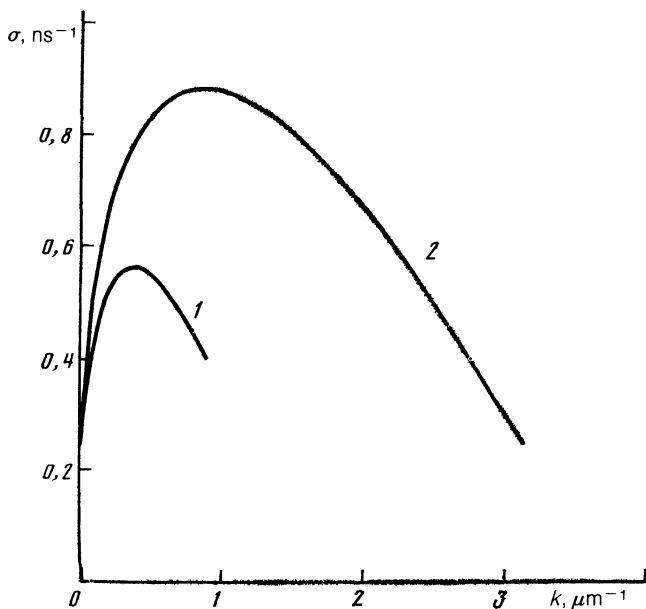


FIG. 6. Instability spectra for the ablative acceleration of an Al target for unperturbed flows corresponding to the profiles in Figs. 1a (curve 1) and 1b (curve 2).

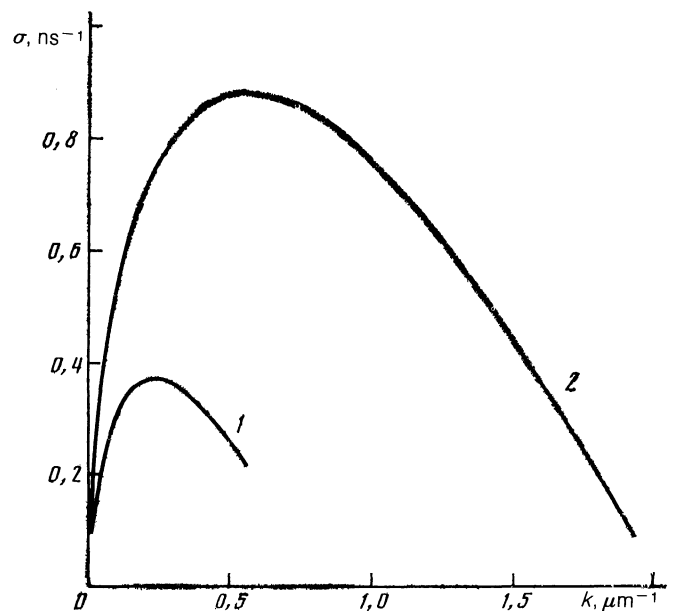


FIG. 7. Instability spectra for the ablative acceleration of an Al target for unperturbed flows corresponding to the profiles in Figs. 2a (curve 1) and 2b (curve 2).

sions  $b$ , the x-ray emission from the plasma corona was artificially suppressed (Figs. 1b and 2b). We then solved the spectral problem (10)–(13) with unperturbed solutions for the case of the irradiation of a target with laser light with  $\lambda_l = 1.06 \mu\text{m}$  (Fig. 6) and  $\lambda_l = 0.26 \mu\text{m}$  (Fig. 7).

It can be seen from the results in Figs. 6 and 7 that the heating of the dense layers of the target by x radiation from the plasma corona causes a substantial decrease in the instability growth rate and a shift of the fastest-growing instability mode into the long-wavelength part of the  $\sigma(k)$  spectrum. Specifically, we find  $\lambda_{\text{max}} \approx 16 \mu\text{m}$  and  $\lambda_{\text{max}} \approx 7 \mu\text{m}$  for laser irradiation with wavelength  $\lambda_l = 1.06 \mu\text{m}$  with and without x radiation from the plasma corona, respectively. We find  $\lambda_{\text{max}} \approx 25 \mu\text{m}$  and  $\lambda_{\text{max}} \approx 16 \mu\text{m}$ , respectively, in the case of laser irradiation with a wavelength  $\lambda_l = 0.26 \mu\text{m}$ .

Figure 8 shows the spectrum of the growth rate of the RT instability for the ablative acceleration of targets by laser light with  $\lambda_l = 0.26 \mu\text{m}$  at intensities  $I = 10^{13} \text{ W/cm}^2$  and  $I = 5 \cdot 10^{12} \text{ W/cm}^2$  under the conditions of the unperturbed flows shown in Figs. 2b and 3, respectively. As expected, under otherwise constant conditions the primary effects of a change in the intensity of the laser light are a change in the acceleration of the target, a change in the convection velocity, and a corresponding change in the instability growth rates.

It was shown in Sec. 4 above that it is not possible, strictly speaking, to find an analytic solution of the problem for the growth rate of RT instabilities with convection of particles through the instability localization region in the very simple model in which the transition region is replaced by a discontinuity front. On the other hand, the spectral problem can be solved numerically, by integration through a transition region with a given (known) structure. Actually, specifying the structure of the discontinuity front, i.e., specifying the spatial distribution of the hydrodynamic variables in the region ( $z_0, z_a$ ), is equivalent to specifying an additional boundary condition in the problem with uniform plas-

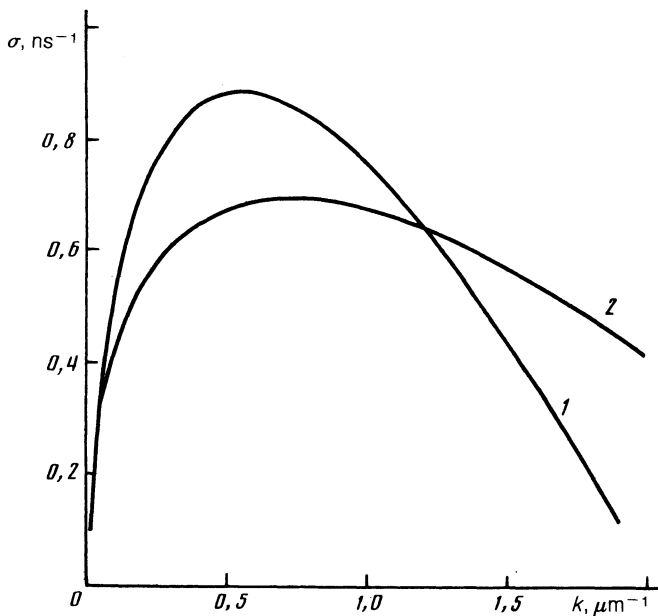


FIG. 8. Instability spectra for the ablative acceleration of an Al target for unperturbed flows corresponding to the profiles in Figs. 2b (curve 1) and 3 (curve 2).

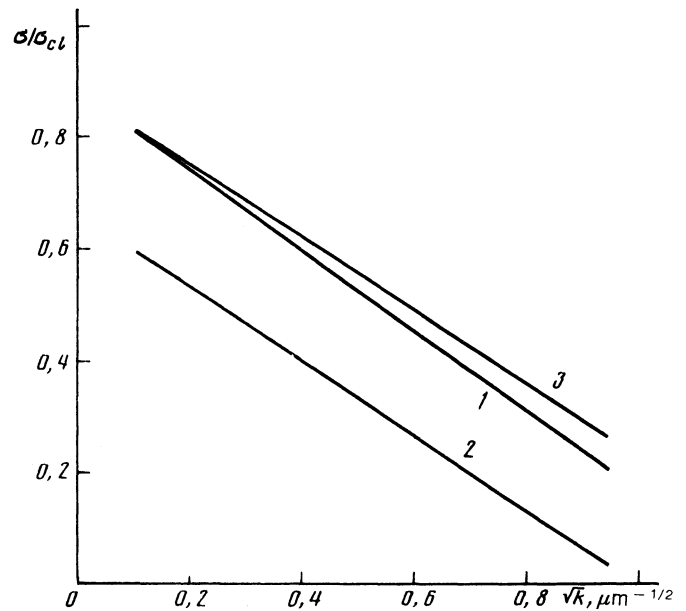


FIG. 10. Ratio of the instability growth rates to  $\sigma_{cl} = (gk)^{1/2}$  for the solution of the spectral problem with boundary conditions (16), (68); for the solution of the spectral problem for the model with a "discontinuity front"; and for the approximation of the 2D simulation on the basis of (1) for the unperturbed flow under the conditions of Fig. 1a.

ma flows separated by a discontinuity front. It is therefore of interest to compare the solution of the "exact" spectral problem with the model problem of the stability of the ablation front. In the latter case, the unperturbed flow used in the solution of spectral problem (10)–(13) was the transition region ( $z_0, z_a$ ) with the structure found from the 1D numerical simulation, but with a uniform plasma flow  $\rho = \rho(z_0) = \text{const}$  at  $z \leq z_0$  and with another uniform plasma flow  $\rho = \rho(z_a) = \text{const}$  at  $z \geq z_a$ . Accordingly, in the spectral problem of the stability of the ablation front, the boundary conditions (16) at the free rear surface of the target were

replaced by the boundary condition that the perturbations of all the quantities in the uniform flows vanish on each side of the discontinuity front and far from it. For  $z > z_a$ , i.e., downstream, these boundary conditions are equivalent to (68), while for  $z < z_0$  the corresponding boundary conditions replacing (16) are

$$\tilde{v}_z = -i\tilde{v}_x, \quad \tilde{P} = -\rho_1 \left( \frac{\sigma}{k} + v_1 \right) \tilde{v}_z, \quad \tilde{p} = \frac{\tilde{P}}{c_s^2}. \quad (69)$$

Figure 9 shows the RT instabilities found through a solution of spectral problem (10)–(13) for a discontinuity front with the boundary conditions (68) and (69). Curve 1 corresponds to the front structure of Fig. 1a, while curve 2 corresponds to the solution of the spectral problem with boundary conditions (68) and (69). Curve 3 is a plot of the approximate expression (1).

Our calculations show that the instabilities found through the solution of the spectral problem for the "actual" unperturbed flow of the plasma of the accelerated target are approximately the same as the results of the 2D numerical simulation for the instability growth rate. The difference in growth rates is less than 20%. The instability growth rates found in the model with a discontinuity front, on the other hand, are in most cases considerably smaller (Fig. 9), although the instability spectra are qualitatively similar.

The instability growth rates for the exact solution of the spectral problem, for the solution for the case of a discontinuity front, and for expression (1) are shown by the curves 1–3, respectively, in Fig. 10 for unperturbed flows under the conditions of Fig. 1a. These growth rates are shown here as ratios formed with the classical value  $\sigma_{cl} = (gk)^{1/2}$ .

## 9. CONCLUSION

This analysis of the growth rate of the RT instabilities in ablatively accelerated laser targets shows that the factor of

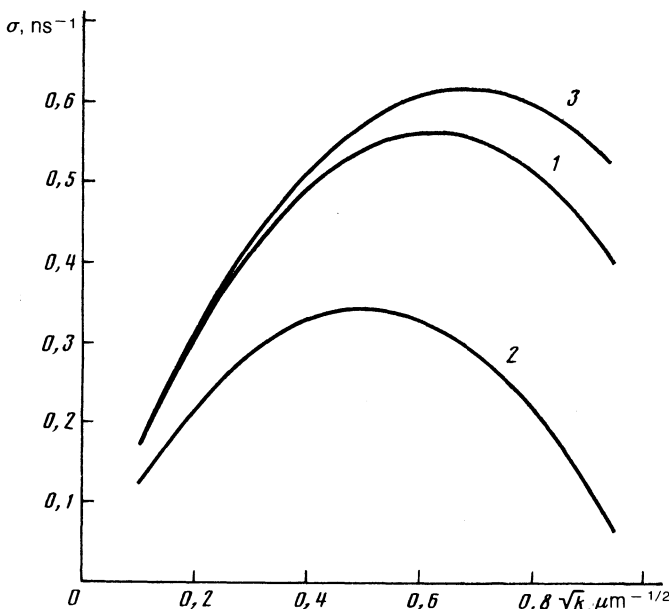


FIG. 9. Instability spectra for the ablative acceleration of an Al target for unperturbed flows corresponding to the profiles in Fig. 1a. 1—Solution of the spectral problem with boundary conditions (16), (68); 2—solution of the spectral problem for the model with a "discontinuity front"; 3—approximation of the 2D simulation on the basis of (1).

primary importance in stabilizing these instabilities is the convection of plasma particles out of the unstable region in the ablation zone ( $z_0, z_d$ ). This convection velocity in turn depends primarily on the laser wavelength and the intensity of the x-ray emission from the plasma corona. As the laser wavelength is reduced, the critical surface moves closer to the ablation front, so the convective transport of particles out of the instability localization region is effectively increased. In addition, the more intense emission of x radiation from the plasma corona causes, as a result of heating, smoothing of the density profiles in the dense layers of accelerated plasma, so the role of the convective removal of particles out of the instability region is effectively strengthened.

The wavelengths of the instability modes which grow most rapidly are  $\lambda_{\max} \approx 25 \mu\text{m}$  and  $\lambda_{\max} \approx 16 \mu\text{m}$  for the ablative acceleration of an aluminum foil with  $d_0 = 10 \mu\text{m}$  irradiated by a laser with  $I = 10^{13} \text{ W/cm}^2$  for laser wavelengths  $1.06 \mu\text{m}$  and  $0.26 \mu\text{m}$ , respectively. If, on the other hand, the spectra found for the instability growth rates are limited to  $\sigma \gg 1/\tau_H$  ( $\tau_H \approx 3 \text{ ns}$  is the time scale of the variations in the hydrodynamic properties of the unperturbed flow), we find that the instabilities are "cut off" in the long-wavelength region at  $\lambda \approx 150 \mu\text{m}$  and  $\lambda \approx 50 \mu\text{m}$  and in the short-wavelength region at  $\lambda \approx 5 \mu\text{m}$  and  $\lambda \approx 15 \mu\text{m}$ , respectively, for laser wavelengths of  $1.06 \mu\text{m}$  and  $0.26 \mu\text{m}$ . These results agree satisfactorily with the experimental results of Refs. 3 and 4.

Some interesting opportunities arise from the possibility of changing the growth rate of the RT instabilities by changing the intensity of the x-ray emission from the plasma corona and by changing the dynamics of the accelerated plasma. These changes might be achieved, for example, by using multilayer targets with large- $Z$  layers on the front of the target, as was first pointed out by Gardner *et al.*<sup>8</sup>

The solution of the eigenvalue problem (10)–(13) leads to results which are approximately the same as the results of a direct  $2D$  numerical simulation, but these results are achieved at a much lower cost in computer time. The method proposed here thus makes it possible to derive unperturbed  $1D$  profiles and a system of equations for the perturbations in which the number of important physical processes taken into account is substantially greater than would be possible in a direct numerical simulation of the growth of perturbations. This new approach also simplifies the problem of finding the most important scaling behavior, which is useful for an optimization.

The experimental results presently available agree with the general trends in the behavior of the instability growth rate according to the theory, but the data available are not an adequate basis for making a detailed comparison with the theory.

We wish to thank A. B. Bud'ko, A. L. Velikovich, A. Yu. Gol'tsov, N. G. Koval'skiĭ, M. I. Pergament, S. Bodner, and D. Book for useful discussions.

<sup>1)</sup> The estimate (58) can easily be obtained also for, e.g.,  $\rho v = \text{const}$  (steady unperturbed flow). Qualitatively, Eq. (58) remains unchanged.

<sup>1</sup> S. Chandrasekhar, *Hydrodynamic and Hydromagnetic Stability*, Oxford, Leningrad, 1961.

<sup>2</sup> L. D. Landau and E. M. Lifshitz, *Fluid Mechanics*, Nauka, Moscow, 1986 (Pergamon, Oxford, 1987).

<sup>3</sup> J. Grun, M. E. Emery, C. K. Manka *et al.*, Phys. Rev. Lett. **58**, 2672 (1987).

<sup>4</sup> M. H. Emery, J. H. Gardner, and S. E. Bodner, Phys. Rev. Lett. **57**, 703 (1986).

<sup>5</sup> H. Nishimura, H. Takabe, and K. Mima, Phys. Fluids **31**, 2875 (1988).

<sup>6</sup> J. D. Kilkenny, Phys. Fluids **2**, 1440 (1990).

<sup>7</sup> R. L. McCrory, J. M. Soares, C. P. Verdon *et al.*, Plasma Phys. Contr. Fusion **31**, 1517 (1989).

<sup>8</sup> J. H. Gardner, S. E. Bodner, and J. P. Dahlburg, Phys. Fluids (1991).

<sup>9</sup> M. H. Emery, J. P. Dahlburg, and J. H. Gardner, Phys. Fluids **31**, 1007 (1988).

<sup>10</sup> C. P. Verdon, R. L. McCrory, R. L. Morse *et al.*, Phys. Fluids **25**, 1563 (1982).

<sup>11</sup> M. H. Emery, J. H. Gardner, and J. P. Boris, Phys. Rev. Lett. **48**, 677 (1982).

<sup>12</sup> R. G. Evans, R. J. Bennet, and G. J. Pert, Phys. Rev. Lett. **49**, 1639 (1982).

<sup>13</sup> H. Takabe, L. Montierth, and R. L. Morse, Phys. Fluids **26**, 2299 (1983).

<sup>14</sup> H. Takabe, K. Mima, L. Montierth, and R. L. Morse, Phys. Fluids **28**, 3676 (1985).

<sup>15</sup> S. E. Bodner, Phys. Rev. Lett. **33**, 761 (1974).

<sup>16</sup> L. Baker, Phys. Fluids **21**, 295 (1978).

<sup>17</sup> L. Baker, Phys. Fluids **26**, 950 (1983).

<sup>18</sup> D. G. Colombant and W. H. Manheimer, Phys. Fluids **26**, 3127 (1983).

<sup>19</sup> W. H. Manheimer and D. G. Colombant, Phys. Fluids **27**, 983 (1984).

<sup>20</sup> W. H. Manheimer and D. G. Colombant, Phys. Fluids **27**, 1927 (1984).

<sup>21</sup> H. J. Kull and S. I. Anisimov, Phys. Fluids **29**, 2067 (1986).

<sup>22</sup> H. J. Kull, Phys. Fluids **1**, 170 (1989).

<sup>23</sup> D. L. Book, "Self-consistent analytical treatment of the role of convection in the Rayleigh–Taylor instability of a laser-driven target," Plasma Phys. Controlled Fusion (to be published, 1992).

<sup>24</sup> D. H. Munro, Phys. Rev. A **38**, 1433 (1988).

<sup>25</sup> B. H. Ripin, P. R. Witloche, F. C. Young *et al.*, Phys. Rev. Lett. **43**, 350 (1979).

<sup>26</sup> B. H. Ripin, R. Decoste, S. P. Oberschain *et al.*, Phys. Fluids **23**, 1012 (1980).

<sup>27</sup> L. A. Bol'shov, I. N. Burdonskiĭ, A. L. Velikovich *et al.*, Zh. Eksp. Teor. Fiz. **92**, 2060 (1987) [Sov. Phys. JETP **65**, 1160 (1987)].

<sup>28</sup> I. N. Burdonskiĭ, A. L. Velikovich, V. V. Gavrilov *et al.*, Laser Particle Beams **6**, 327 (1988).

<sup>29</sup> S. J. Gitomer, R. L. Morse, and B. S. Newberger, Phys. Fluids **20**, 234 (1977).

<sup>30</sup> L. H. Montierth and R. L. Morse, Phys. Fluids B **2**, 353 (1990).

<sup>31</sup> H. Hora, in *Laser Interaction and Related Plasma Phenomena*, Plenum, New York, 1971.

<sup>32</sup> A. V. Bushman, G. I. Kanel', A. L. Hi, and V. E. Fortov, *Thermal Physics and Dynamics of Intense Pulsed Processes*, Chernogolovka, 1988.

<sup>33</sup> S. Atzeni, Plasma Phys. Contr. Fusion **29**, 1535 (1987).

<sup>34</sup> A. L. Velikovich and M. A. Liberman, *Physics of Shock Waves in Gases and Plasmas*, Nauka, Moscow, 1987.

<sup>35</sup> N. A. Inogamov, Zh. Prikl. Mekh. Tekh. Fiz. **5**, 110 (1985).

<sup>36</sup> A. B. Bud'ko, A. L. Velikovich, M. A. Liberman, and F. S. Felber, Zh. Eksp. Teor. Fiz. **96**, 140 (1989) [Sov. Phys. JETP **69**, 76 (1989)].

<sup>37</sup> V. V. Bychkov, M. A. Liberman, and A. L. Velikovich, Phys. Rev. A **42**, 5031 (1990).

<sup>38</sup> L. D. Landau and E. M. Lifshitz, *Quantum Mechanics: Non-Relativistic Theory*, Nauka, Moscow, 1989 (previous editions of this book have been published in English translation by Pergamon, New York).

Translated by D. Parsons